Backbone and Side-Chain ^{13}C and ^{15}N Signal Assignments of the α-Spectrin SH3 Domain by Magic Angle Spinning Solid-State NMR at 17.6 Tesla

Jutta Pauli,[b] Marc Baldus,*[a] Barth van Rossum,[b] Huub de Groot,[a] and Hartmut Oschkinat*[b]

The backbone and side-chain ^{13}C and ^{15}N signals of a solid 62-residue (u-^{13}C,^{15}N)-labelled protein containing the α-spectrin SH3 domain were assigned by two-dimensional (2D) magic angle spinning (MAS) $^{15}N-^{13}C$ and $^{13}C-^{13}C$ dipolar correlation spectroscopy at 17.6 T. The side-chain signal sets of the individual amino acids were identified by 2D $^{13}C-^{13}C$ proton-driven spin diffusion and dipolar recoupling experiments. Correlations to the respective backbone nitrogen signals were established by 2D NCACX (CX = any carbon atom) experiments, which contain a proton–nitrogen and a nitrogen–carbon cross-polarisation step followed by a carbon–carbon homonuclear transfer unit. Interresidue correlations leading to sequence-specific assignments were obtained from 2D NCOCX experiments. The assignment is nearly complete for the SH3 domain residues 7–61, while the signals of the N- and C-terminal residues 1–6 and 62, respectively, outside the domain boundaries are not detected in our MAS spectra. The resolution observed in these spectra raises expectations that receptor-bound protein ligands and slightly larger proteins (up to 20 kDa) can be readily assigned in the near future by using three-dimensional versions of the applied or analogous techniques.

KEYWORDS:

NMR spectroscopy · protein structures · SH3 domains · solid-state structures · spectrin

Introduction

Structure determination of membrane-integrated protein systems is in the centre of scientific interest due to their importance in signalling processes and human diseases. Structural information on, for example, peptide agonists or antagonists bound to G-protein-coupled receptors would be a tremendous help for understanding the initiation of vital signalling events. Solid-state magic angle spinning (MAS) NMR[1, 2] is rapidly forthcoming as a tool for structural studies of such ligand–protein interactions involving membrane proteins. A major prerequisite for structural studies on solid proteins is the development of methods for obtaining full ^{13}C,^{15}N signal assignments using a uniformly labelled solid protein sample. There are a number of nontrivial experimental problems that need to be considered in this context. Unlike in the liquid state, chemical shielding interactions or dipolar couplings are strong and anisotropic in solid protein samples and can be of comparable size or exceed the strength of the applied radio frequency (r.f.) field. It is thus important to apply MAS pulse schemes that allow to select and resolve characteristic backbone and side-chain ^{15}N,^{13}C spin topologies without undesirable dipolar coupling or truncation effects. These topologies may be studied by various combinations of heteronuclear[3–6] and homonuclear correlation methods,[7–11] possibly augmented by selective excitation or decoupling. Additional restrictions resulting from limitations in hardware performance and from the general sensitivity of the protein structure to high MAS frequencies or probe temperatures need to be considered with equal importance. We have thus concentrated on pulse schemes that can be employed at medium r.f. fields while using moderately fast MAS. All selected techniques and combinations thereof might be applied in a two- (2D) or three-dimensional (3D) manner. For a number of reasons, protein assignment concepts in solid-state NMR are intrinsically different to those known from solution NMR. There, triple-resonance experiments like HNCO, HNCA, CBCANNH, CBCA(CO)NNH, HBHA(CBCA)NNH and HBHA(CBCACO)NNH[12–16] are

[a] *Dr. M. Baldus,[+] Prof. H. de Groot*
Gorlaeus Laboratories
University of Leiden
P.O. Box 9502, 2300 RA Leiden (The Netherlands)

[b] *Prof. H. Oschkinat, Dr. J. Pauli, Dr. B. van Rossum*
Forschungsinstitut für Molekulare Pharmakologie
Robert-Rössle-Strasse 10, 13125 Berlin (Germany)
Fax: (+49) 30-94793-169
E-mail: oschkinat@fmp-berlin.de

[+] *Present address:*
Max Planck Institute for Biophysical Chemistry
Solid-state NMR
Am Fassberg 11, 37077 Göttingen (Germany)
Fax: (+49) 551-201-1320
E-mail: maba@mpibpc.mpg.de

  1439-4227/01/02/04 $ 17.50+.50/0 CHEMBIOCHEM **2001**, 2, 272–281

routinely used as three-dimensional techniques involving proton detection. However, proton detection in solid-state NMR is yet challenging even with high-frequency MAS. In addition, existing techniques for line narrowing during the ^{1}H detection period presently do not yield large sensitivity enhancements. For this reason, the techniques used for assignment of proteins with MAS solid-state NMR will likely involve detection of ^{13}C or ^{15}N signals. Applications of the frequency-switched Lee – Goldburg technique[17, 18] at high field for line narrowing of proton signals in a virtual dimension are promising, although the signals are still not as well resolved as in solution.[19] Interresidue correlations will therefore be dominantly obtained by combinations of heteronuclear band-selective ^{15}N – ^{13}C cross-polarisation (CP) and homonuclear ^{13}C – ^{13}C dipolar recoupling techniques, while protons can be observed, if desired, by indirect detection using the frequency-switched Lee – Goldburg decoupling technique.[19]

Along these lines, we have obtained a relatively complete assignment of the ^{13}C and ^{15}N signals of the 62-residue α-spectrin SH3 domain, except the flexible N- and C termini of the 62-residue construct used (MDETG KELVL ALYDY QEKSP REVTM KKGDI-LTLLN STNKD WWKVE VNDRQ GFVPA AYVKK-LD), whose signals were not detected in the MAS spectra. This was achieved by a suitable combination of heteronuclear and homonuclear 2D MAS NMR techniques. The presented concept might be useful in the structure determination process of both receptor-bound hormones and moderately sized membrane-integrated proteins.

Results

The data set

The data set comprised 2D ^{13}C – ^{13}C correlation experiments employing proton-driven spin diffusion (PDSD)[20] and dipolar recoupling by using the radio-frequency-driven dipolar recoupling (RFDR) sequence.[7] The latter spectra were obtained as previously described.[21] Both techniques are easy to implement and have successfully been applied to multi-labelled ^{13}C spin systems.[21–24] We investigate in the following the transfer characteristics of both methods under MAS at 17.6 T. We did not test other ^{13}C – ^{13}C correlation experiments, since all expected cross peaks were found in our spectra. Band-selective nitrogen – carbonyl (NCO) and nitrogen – C$^{\alpha}$-carbon (NCA) correlations were collected with the SPECIFIC-CP sequence[6] (Figure 1 a), and two relayed sequences, generated by extending the NCA and NCO sequences (Figure 1 a) with different carbon – carbon transfer steps (Figure 1 b and c). The sequence shown in Figure 1 b contained a proton-driven spin diffusion unit for carbon – carbon mixing and was used to record NCACX and NCOCX spectra. The sequence shown in Figure 1 c, which employs a band-selective polarisation transfer under DREAM[25] (BASE-DREAM) to achieve carbon – carbon transfer via a double-quantum mixing unit,

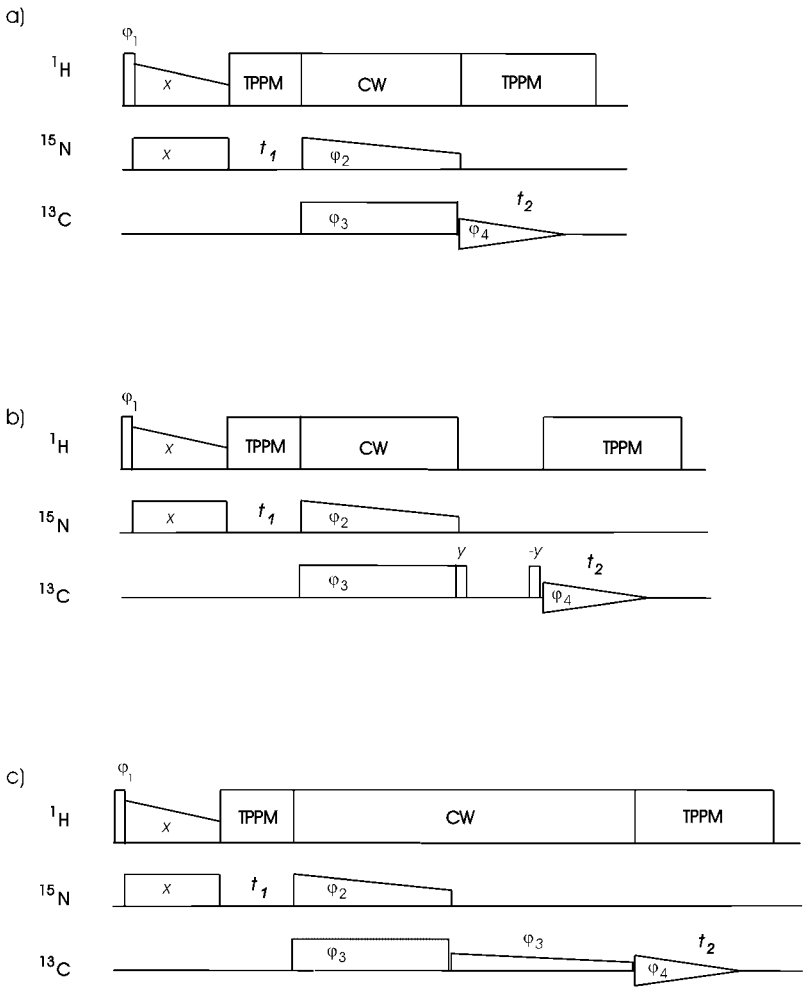

Figure 1. *Pulse sequences for the ^{15}N – ^{13}C correlation spectroscopy used in this work. In all cases, ramped[35, 36] proton r.f. fields were used to prepare ^{15}N polarisation via a broad-band (^{1}H,^{15}N) CP transfer. TPPM decoupling[39] was applied during evolution and detection. a) Band-selective ^{15}N – ^{13}C polarisation transfer was used to record the NCO and NCA spectra shown in Figure 2, which was achieved by applying r.f. fields of 30 kHz (^{15}N) and 15 kHz (^{13}C), respectively. The ^{13}C carrier frequency was centred at $\delta = 45$ (NCA) and $\delta = 185$ (NCO). During the heteronuclear ^{15}N – ^{13}C CP a linear ramp (100 – 80 %) was applied on the ^{15}N channel to optimise efficiency and selectivity of the transfer. b) ^{15}N – ^{13}C correlation transfer with a ^{13}C – ^{13}C mixing unit used to record the NCACX and NCOCX spectra (see Figures 3 and 4). CA and CO polarisation was prepared as described above followed by proton-driven spin diffusion times of 10 ms (NCACX) or 8 and 30 ms (NCOCX). For excitation and reconversion of longitudinal magnetisation, two 90-degree pulses were applied at a ^{13}C offset frequency of $\delta = 100$ using r.f. fields of 50 kHz. c) ^{15}N – ^{13}C correlation transfer with a double-quantum mixing unit to achieve carbon – carbon transfer (Figure 4, bottom). The sequence was used to record an NCACX-BD spectrum. Double-quantum mixing was achieved by a weak ^{13}C B_1 field that was linearly amplitude-modulated from 6 to 3 kHz during a mixing time of 2 ms. The following phase cycles were applied: φ_1 = y, y, −y, −y; φ_2 = x, −x, x, −x, −x, x, −x, x; φ_3 = x, x, x, x, −x, −x, −x, −x; φ_4 = x, −x, −x, x.*

served for obtaining an NCACX spectrum with a different transfer profile.

The $^{13}C-^{13}C$ homonuclear correlation spectra were recorded with mixing times of 5 and 15 ms (PDSD) and 1 and 3 ms (RFDR). In the set of short mixing times (PDSD 5 ms, RFDR 1 ms), cross peaks between the directly bonded carbon atoms were predominantly observed, while for mixing times of 15 and 3 ms, respectively, intraresidue-relayed cross peaks emerged. For reasons of sample sensitivity and hardware limitations, the RFDR technique was only applied in a band-selective manner on the aliphatic region. Therefore, a larger number of correlations between the carbonyl carbon atoms and the aliphatic carbon atoms were only observed in the PDSD spectrum recorded with a mixing time of 15 ms at a 17.6-T spectrometer. Apart from this difference, spectra with equivalent cross peak patterns in the aliphatic regions were obtained by both techniques. The RFDR spectrum recorded with band-selective excitation of the aliphatic region and with a mixing time of 1 ms shows the same cross peaks as found in the aliphatic region of the PDSD spectrum with a mixing time of 5 ms. In addition, the cross peak pattern observed in the RFDR spectrum recorded with a mixing time of 3 ms is identical to the cross peak pattern seen in the aliphatic region of the PDSD spectrum that was measured with a mixing time of 15 ms. It should be noted that these results have been obtained under different experimental conditions from those described in ref. [24].

The NCA and NCO spectra were recorded with band-selective SPECIFIC CP[6] transfer steps. Unlike the conventional CP experiment,[26, 27] SPECIFIC CP is characterised by low- to medium-size r.f. fields that facilitate polarisation transfer whenever the effective field of r.f. irradiation (ω_1, ω_2) and chemical shift offsets (Ω_1, Ω_2) of a heteronuclear spin pair fulfil the following (zero-quantum (ZQ), $n = +1, +2$) recoupling condition [Eq. (1)]:

$$\sqrt{\omega_1^2 + \Omega_1^2} - \sqrt{\omega_2^2 + \Omega_2^2} = n\,\omega_R \qquad (1)$$

Using a slow r.f. amplitude modulation for one of the two r.f. fields (e.g. $\omega_1(t)$), the recoupling condition of Equation (1) can be fulfilled for a defined range of chemical shift offsets. Further theoretical considerations on how to select the applied r.f. fields ω_1 and ω_2 or the resonance offsets Ω_1 and Ω_2 in Equation (1) and how to maximise the transfer efficiency for a given MAS frequency ω_R can be found in ref. [6]. This concept was applied to obtain NCA and NCO spectra containing exclusively $N_iC_i^{\alpha}$ and N_iCO_{i-1} cross peaks (Figure 2), respectively, which provide a high-resolution fingerprint of the protein. They are particularly useful for distinguishing direct and relayed correlations in the NCACX and NCOCX spectra discussed below. The NCO and NCA spectra were recorded at a MAS frequency of 12 kHz and with a proton decoupling field of 100 kHz to enhance resolution. The same band-selective N–C transfer was used as a preparatory unit for recording NCACX and NCOCX spectra of sufficient selectivity and intensity. For the carbon–carbon correlation step contained in these experiments we have applied two complementary schemes taking into consideration the hardware and sample requirements discussed above. The first scheme exploits again spectral spin diffusion during MAS (Figure 1 b). Unlike 2D $^{13}C-^{13}C$-correlation experiments, the selective preparation of CA or CO

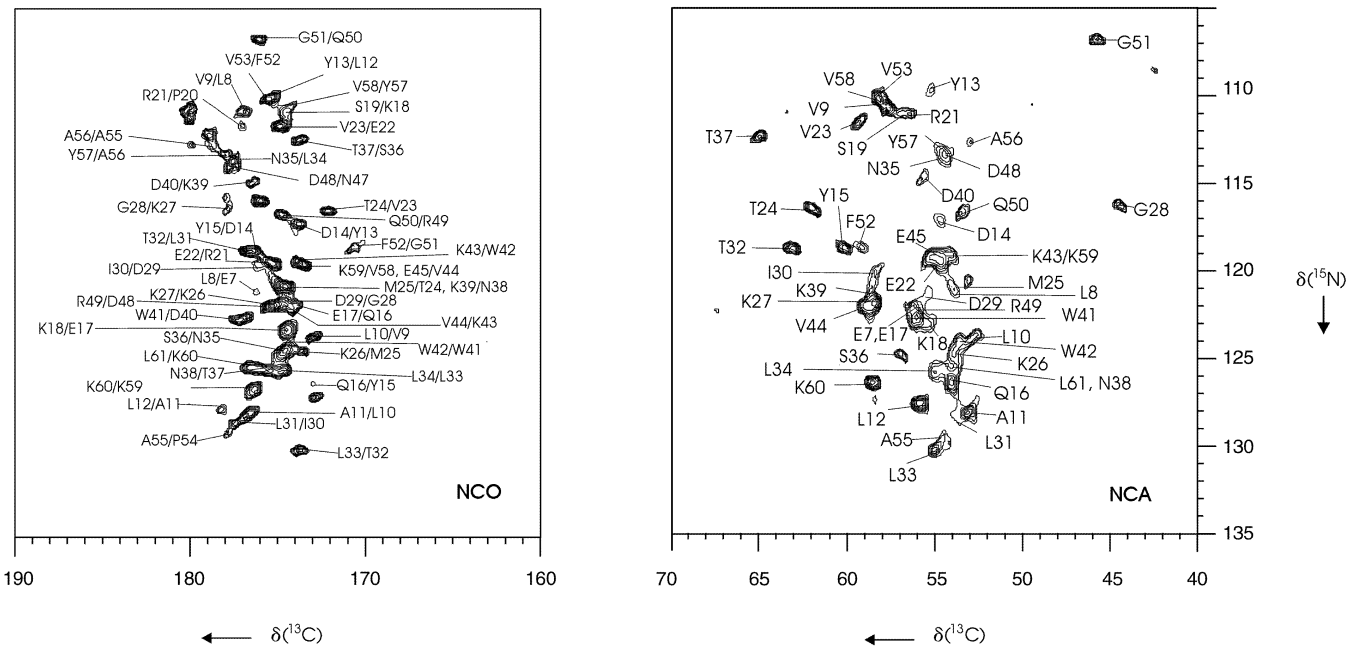

Figure 2. NCO (left) and NCA (right) spectra of the precipitated α-spectrin SH3 sample recorded with the pulse sequence shown in Figure 1 a with appropriate settings for carbon power and frequency. The spinning frequency was 12 kHz, and the temperature was adjusted to 278 K. Assigned signals are indicated with the respective residue type and number. In the spectrum at the left, the NCO cross peaks yielding sequential information are indicated with the residue contributing to the nitrogen chemical shift first, followed by the residue that contributes to the carbonyl chemical shift. Both spectra were processed to yield optimal resolution by applying a phase shifted by π/3 sine-bell function in t_1 and a Lorentz–Gauss transformation in t_2.

polarisation leads to different transfer characteristics due the homonuclear correlation unit. In our applications of the PDSD mixing technique in NCACX experiments at 17.6 T and 8-kHz MAS, we observed an preferred transfer between the C^{α} atom and those carbon atoms with signals in the region between $\delta = 20$ and $\delta = 35$. This is expected from theoretical investigations[28–30] since the chemical shift differences Δ match a multiple of the spinning frequency, that is, $\Delta = n\omega_R$ ($n = 1, 2\ldots$). Such a preferred transfer was never observed in 2D $^{13}C-^{13}C$-correlation experiments with mixing times between 1 ms and 15 ms (Figure 3, top).

The second approach (Figure 1 c) involves a homonuclear double-quantum (DQ) transfer unit and is optimised for band-selective transfer in small- to medium-size chemical shift ranges (in our case: between 65 – 30 ppm). The concept is based on an amplitude-modulated version of the continuous-wave (CW) recoupling experiment HORROR,[31] originally proposed to measure interatomic distances, and can also be applied in the context of DREAM ultrafast MAS double-quantum filtering.[25] For our experimental conditions and requirements we wish to establish band-selective transfer over a defined frequency range and thus use the term band-selective polarisation transfer under DREAM (BASE-DREAM). Similar to the ZQ condition for SPECIFIC CP transfer, double-quantum transfer is possible if the r.f. field $\omega_{r.f.}$ and the offsets, Ω_1 and Ω_2, fulfil the following condition [Eq. (2)]:

$$\sqrt{\omega_{r.f.}^2 + \Omega_1^2} + \sqrt{\omega_{r.f.}^2 + \Omega_2^2} = n\omega_R \quad (2)$$

Band selectivity is again achieved by a slow amplitude modulation, $\omega_{r.f.} \rightarrow \omega_{r.f.}(t)$. MAS frequency and offsets were chosen to cover a chemical shift range of less than 40 which allows for the selective observation of $C^{\alpha}-C^{\beta}$ correlations of those amino acids whose C^{β} signals occur between $\delta = 30$ and $\delta = 45$. Placing the r.f. carrier around $\delta = 45$ extends the observation window for C^{β} signals up to $\delta = 65$ (Ser). The transfer leads to negative intensities on C^{β} signals and simplifies the analysis of the correlation pattern.[8]

In Figure 3 (bottom) and Figure 4 subspectra of the NCACX experiments are shown. The NCACX spectrum (Figure 4, top, blue) was recorded with a proton-driven spin diffusion mixing sequence employing a mixing time of 10 ms, and the NCACX spectrum shown in Figure 4 (bottom) with a BASE-DREAM sequence. The two techniques will be henceforth called NCACX-PDSD and NCACX-BD. In case of the NCACX-PDSD sequence, a spectrum with stronger relayed cross peaks involving the C^{β} and C^{γ} signals around $\delta = 15-40$ was obtained, whereas in the NCACX-BD experiment such kind of relayed cross peaks occurred exclusively in the ^{13}C chemical shift range of $\delta = 25-45$. The latter observation fully agrees (for the 2-ms mixing time employed) with our theoretical expectation according to Equation (2). Furthermore, cross peaks of the type N_iCO_i are only observed in the NCACX-PDSD spectrum, and not in the NCACX-BD spectrum.

Two NCOCX experiments containing a broad-band carbon – carbon transfer step after the selective nitrogen – carbon cross polarisation period were recorded for obtaining interresidue correlations. Carbon – carbon mixing was achieved with a unit employing proton-driven spin diffusion for mixing times of 8 and 30 ms, the latter shown in Figure 4 (top, red). As a result, signals at the F2 positions of CO, C^{α}, C^{β} and C^{γ} of residue i are correlated with the nitrogen signal of residue $i+1$. Experimental parameters were tuned for a selection of cross peaks of the type $N_{i+1}CO_i$, $N_{i+1}C_i^{\alpha}$, $N_{i+1}C_i^{\beta}$ and $N_{i+1}C_i^{\gamma}$, while signals of the type N_iC_i were suppressed. This selectivity of the nitrogen – carbon transfer is important for avoiding misassignments.

Assignment strategies

The set of experiments presented above offers several possibilities for generating sequential assignments, which are shown in Figure 3 and Figure 4. Side-chain assignments that were obtained from the $^{13}C-^{13}C$ PDSD spectrum were included at each step of the sequential assignment procedure to increase reliability. As an example, the signal pattern of a threonine residue (T32) in a PDSD spectrum recorded with a mixing time of 15 ms is shown in Figure 3 (top, dashed lines). In this case, an unequivocal identification of the C^{α}, C^{β}, C^{γ} and CO chemical shifts and therefore of the amino acid type is possible due to the characteristic chemical shift of the β-carbon signal at $\delta = 69.8$.[21, 23, 24] To facilitate the sequential assignment, it is important to identify also the chemical shift of the backbone nitrogen atom of the respective residue. This can be achieved by comparing the signal pattern identified in the carbon – carbon correlation spectra (Figure 3, top) with the NCACX-PDSD spectrum (Figure 3, bottom right), that contains signals of the type N_iCO_i, $N_iC_i^{\alpha}$, $N_iC_i^{\beta}$ and in favourable cases also $N_iC_i^{\gamma}$ for most of the residues. The identification of the nitrogen chemical shift of T32, for instance, is indicated in the NCACX-PDSD spectrum by the prolongation of the dashed lines drawn into the PDSD spectrum. The spectral region shown in the lower left corner of Figure 3 is taken from an NCOCX spectrum in which no cross peaks of the type N_iCO_i occur, therefore the position of $N_{T32}CO_{T32}$ has been indicated by a cross.

The simplest procedure to obtain sequential assignments involves the comparison of the 2D NCACX and 2D NCOCX spectra, which are shown as a superposition in blue and red colours, respectively, in Figure 4 (top). In the NCACX spectrum (blue), the cross peaks of a particular residue i with a unique side-chain topology may serve as starting points. These cross peaks are of the types N_iCO_i, $N_iC_i^{\alpha}$, $N_iC_i^{\beta}$ and $N_iC_i^{\gamma}$. The involved carbon chemical shifts are found at a different nitrogen frequency in the NCOCX spectrum (red). This nitrogen frequency is the position of the amide nitrogen signal of the residue following in the sequence. There, cross peaks of the type $N_{i+1}CO_i$, $N_{i+1}C_i^{\alpha}$, $N_{i+1}C_i^{\beta}$ and $N_{i+1}C_i^{\gamma}$, respectively (red), occur. In a graphical assignment procedure, the respective types of cross peaks (e.g. N_iCO_i (blue) and $N_{i+1}CO_i$ (red), $N_iC_i^{\alpha}$ (blue) and $N_{i+1}C_i^{\alpha}$ (red), and $N_iC_i^{\beta}$ (blue) and $N_{i+1}C_i^{\beta}$ (red)) could be connected by vertical lines. An example are the correlations between the G51 auto peaks ($N_{G51}CO_{G51}$ and $N_{G51}C_{G51}^{\alpha}$, blue) and the sequential peaks involving the F52 nitrogen atom ($N_{F52}CO_{G51}$ and $N_{F52}C_{G51}^{\alpha}$, red) in the two top frames in Figure 4. The next step is the identification of cross peaks of the type $N_{i+1}CO_{i+1}$, $N_{i+1}C_{i+1}^{\alpha}$, and $N_{i+1}C_{i+1}^{\beta}$ in the NCACX

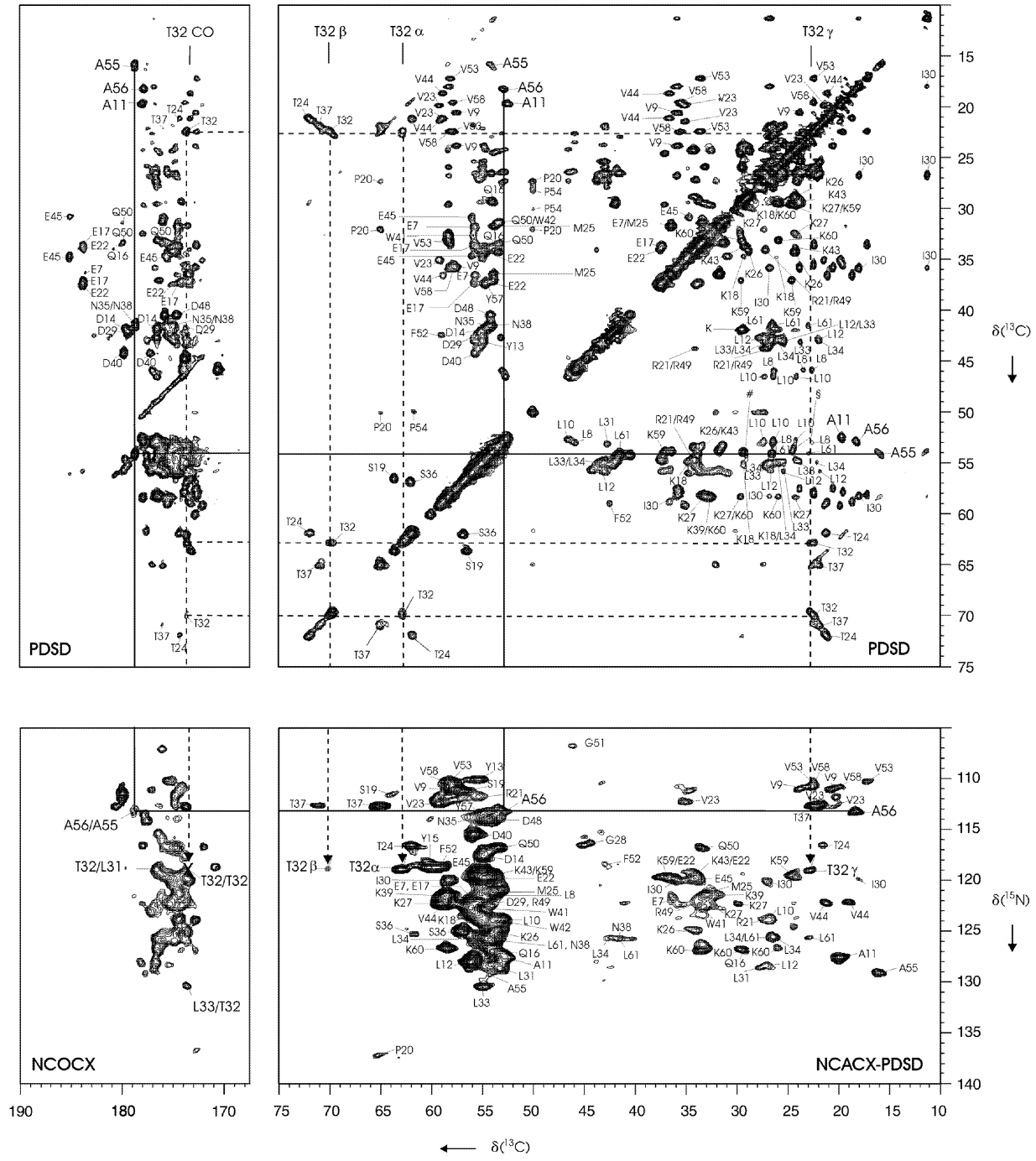

Figure 3. *Top: Two regions from a proton-driven spin diffusion spectrum recorded at a ^{13}C frequency of 188 MHz with a spin diffusion period of 15 ms. The region shown in the left panel contains cross peaks involving the aliphatic carbon atoms and carbonyl carbon atoms, and the right panel shows cross peaks between aliphatic carbon atoms. The signal sets of the prolines, five out of the six valines, four out of the five glutamic acids, the two glutamines, two out of three asparagines, four out of the five aspartic acids, the aromatic residues and the methionine are indicated above the diagonal in the aliphatic region of the PDSD spectra (right panel) by the amino acid type and sequential number. The isoleucine, the leucines, the lysines and the arginines are indicated below the diagonal. Finally the alanines, three out of the four threonines and the serines are shown in a symmetrical manner. # indicates L61, K26, K43, K59. § indicates K26, K43, K59. In the aliphatic/carbonyl region (left panel), cross peaks originating from the glutamic acids, the glutamines, the aspartic acids and the asparagines are indicated that were used for the identification of their amino acid type. Also, the C^{α}/CO and C^{β}/CO cross peaks of three threonines and the C^{β}/CO cross peaks of the three alanines are labelled. Bottom: Left panel: NCO region of the NCOCX spectrum that shows interresidue nitrogen – carbonyl correlations. A cross (X) at $\delta = 118.8/173.8$ indicates the position of the intraresidue cross peak of T32, as observed in the NCO region of the NCACX spectrum (see text for details). Right panel: Aliphatic region of the NCACX spectrum recorded with a PDSD carbon – carbon mixing time of 10 ms. All spectra shown were measured at a spinning frequency of 8 kHz and at a temperature of 278 K. Moderate proton decoupling fields of 70 kHz were applied in all cases. Different contour levels were chosen for the plots of the two regions shown in the bottom part, and in comparison to Figure 2. The signal pattern of threonine 32 is indicated with dashed lines in the PDSD spectra (top), and extended to the NCACX spectrum for locating the T32 nitrogen signal. The two interresidue cross peaks of T32, $N_{T32}CO_{L31}$ and $N_{L33}CO_{T32}$, are also indicated in the NCO region of the NCOCX spectrum. The solid lines connecting A55 and A56 illustrate how sequential assignments can be obtained from the spectral regions in the figure (see text for details).*

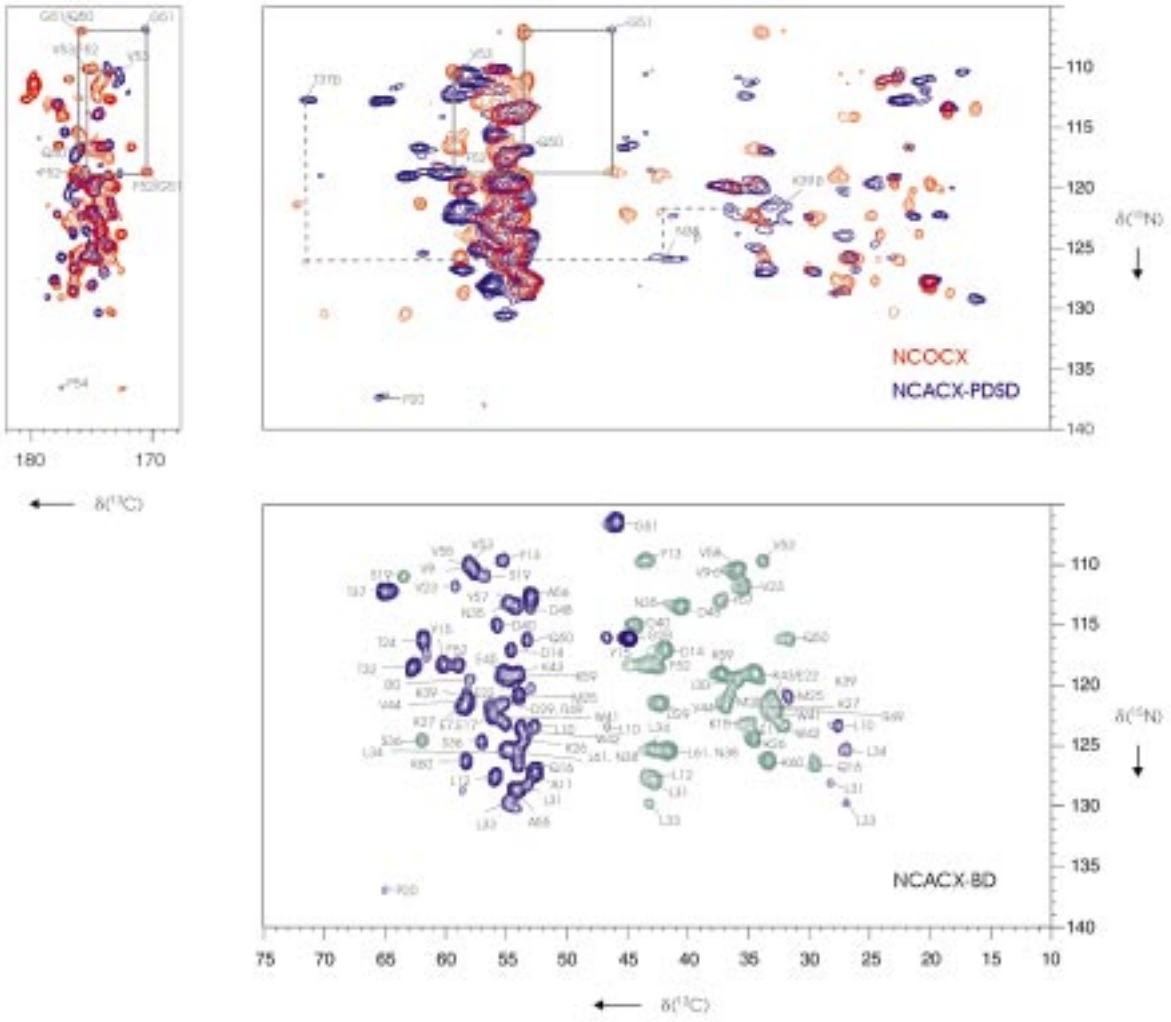

Figure 4. *Top: Superposition of the NCACX-PDSD (blue) and NCOCX (red) spectra of the α-spectrin SH3 protein. The two spectral regions shown have been processed with different window functions and are plotted at different levels for convenient comparison. The aliphatic regions of the NCACX-PDSD and NCOCX spectra were processed by applying a phase shifted by π/3 sine-bell window function in* t_1 *and a Lorentz – Gauss transformation in* t_2*. The carbonyl region was processed such that optimal resolution is obtained by applying a phase shifted by π/3 sine-bell window function in* t_1 *and by a phase shifted by π/2 sine-square window function in* t_2*. Bottom: The aliphatic region of the NCACX-BD spectrum recorded with the BASE-DREAM sequence is shown together with the assignments. Blue peaks are positive, green peaks are negative. The spectra were recorded with a spinning frequency of 8 kHz and at a temperature of 278 K. Correlations used for the sequential assignment are shown in the two spectra in the top part (see text for details).*

spectra (blue) as outlined above. They can be found also in a graphical assignment procedure, where horizontal lines would connect the cross peaks $N_{i+1}CO_i$ (red) and $N_{i+1}CO_{i+1}$ (blue), $N_{i+1}C_i^{\alpha}$ (red) and $N_{i+1}C_{i+1}^{\alpha}$ (blue), and $N_{i+1}C_i^{\beta}$ (red) and $N_{i+1}C_{i+1}^{\beta}$(blue), all on the frequency of the nitrogen signal of residue $i+1$. This is exemplified by the assignment of the α-carbon atoms and the carbonyl groups of G51 and F52 at the nitrogen chemical shifts of G51 and F52 in Figure 4 (top). Similar correlations involving C^{β} cross peaks of the type $N_iC_i^{\beta}$, $N_{i+1}C_i^{\beta}$ and $N_{i+1}C_{i+1}^{\beta}$ are shown in Figure 4 (top) for the sequence stretch T37 →K39. In practical cases it is also useful to execute this procedure in a backwards manner.

An alternative approach for sequential assignment is outlined in Figure 3. The required correlations between C_i^{α}, CO_i, N_{i+1} and C_{i+1}^{α} may be in principle individually detected by means of cross peaks of the type $C_i^{\alpha}CO_i$ in the CACO region of the PDSD spectrum (Figure 3, top left), and $N_{i+1}CO_i$ and $N_{i+1}C_{i+1}^{\alpha}$, taken for example from NCO and NCA spectra, or the respective relayed techniques NCOCX (Figure 3, bottom left) and NCACX (Figure 3, bottom right). The required side-chain information is then available from the aliphatic region of the PDSD spectrum. An example is shown in Figure 3 (solid lines) where the residue pair A55-A56 of the SH3 domain is assigned. The carbonyl signal involved in the cross peak $N_{A56}CO_{A55}$ as observed in the NCO region of the NCOCX spectrum (Figure 3, bottom left) was determined to belong to an alanine because of the characteristic cross peak at $\delta = 15.9/178.7$ ($C_{A55}^{\beta}CO_{A55}$) in the aliphatic/carbonyl region of the PDSD spectrum (Figure 3, top left). The conclusion that the respective NCO cross peak contains the nitrogen chemical shift of A56 is drawn on the basis of the $N_{A56}C_{A56}^{\beta}$ cross peak at $\delta = 113.0/18.2$ observed in the NCACX-PDSD spectrum (Figure 3, bottom right). In practical cases this procedure may be used to help to confirm the sequential assignments obtained by the method described above.

Assignment of the α-spectrin SH3 domain

The 2D RFDR spectra with mixing times of 1 and 3 ms and the proton-driven spin diffusion spectra with mixing times of 5 and 15 ms served for the identification of the signal patterns of all six valines, the isoleucine, the two prolines, the two tryptophans, the phenylalanine, the seven leucines, six lysines, one methionine, the three alanines, the two serines and three threonines. Many assigned cross peaks are indicated in Figure 3 (top right). For most of these amino acids the chemical shifts of the carbonyl signals could be identified by relayed cross peaks in the PDSD spectrum involving the C^{β} and C^{γ} signals. The signal pattern of six glutamines/glutamates and five asparagines/aspartates were revealed by the correlations between their side-chain carbonyl group signals and their C^{γ}, C^{β} and C^{α} signals (Figure 3, top left). The signal sets corresponding to four out of six aromatic residues (the two tryptophans, the phenylalanine and one of the three tyrosines) were identified by the characteristic signal pattern of their aromatic rings and the correlations involving C^{β} signals.

Well-resolved peaks in the NCO and NCA spectra (Figure 2) yielded several starting points for the sequential assignment procedure. Additionally, they allowed for distinction of relayed and direct peaks in the NCACX-type spectra exemplified by the two glycine carbon peaks in the NCA spectrum around $\delta = 45-46$. Due to their distinct C_i^{α} chemical shifts, those peaks were readily assigned to glycines, while at the same time their sequential assignment was simplified due to the isolated position of each peak in the carbon range. In a similar manner, the resolved peaks between $\delta = 60-65$ provided unambiguous correlations along the carbon axis. Since these signals originated from threonines, serines and prolines, of which relatively few are present in the α-spectrin SH3 domain, these correlations yielded the first pairs of sequentially assigned amino acids. Both spectra in Figure 2 served also as a control for the selectivity of the N – C transfer in the NCACX and NCOCX experiments. Those peaks that occur in the NCO spectrum, for example, should not occur in the NCO region of the NCACX spectrum, while the peaks from the NCA spectrum should not be observed in the NCA region of the NCOCX spectrum.

The first step in the evaluation of the NCACX spectra concerned the identification of the amino acid types by comparison with the RFDR and PDSD correlations using the method shown in Figure 3. Most easily found were threonine signal patterns due to the correlation involving the C^{β} signal around $\delta = 70$ (Figure 4, top right, blue signals) and the two serine patterns due to the negative peaks involving the C^{β} signal around $\delta = 64$ and $\delta = 62$ in the NCACX-BD spectrum (Figure 4, bottom, green signals). There are also weak correlations resulting from the two prolines at nitrogen chemical shifts of around $\delta = 137$. In both NCACX spectra (Figure 4, top (blue) and bottom), the signal sets of three threonines, two serines, three alanines, five out of the six valines, the isoleucine and the phenylalanine were easily identified due to the distinct chemical shifts involved.

The sequential assignment procedure was started by establishing interresidue correlations involving those signal sets (including also nitrogen chemical shifts) that were well identified. Serines, prolines and two threonines were then sequentially assigned by correlations of the type $N_{i+1}CO_i$, $N_{i+1}C_i^{\alpha}$ and $N_{i+1}C_i^{\beta}$, yielding the pairs P20/S19, T37/S36, T24/V23 and P54/V53. The three alanines were assigned sequentially by the A56/A55 correlation as shown in Figure 3, and the two glycines by the F52/G51 correlation (Figure 4, top). This yielded six assigned pairs of residues and also the sequence-specific assignment of A11.

The next step involved the prolongation of the assigned fragments. The G51/F52 pair, for example, was extended on the basis of correlations in the NCA and NCO regions, as shown in Figure 4 (top). This lead to the identification of Q50 and V53, and together with the identified pairs V53/P54 and A55/A56 to the assigned sequence fragment Q50 – A56. Subsequently, fragments containing the pairs S36/T37 and V23/T24 were deduced in a similar manner. The importance of correlations of the type $N_iC_i^{\beta}$ and $N_{i+1}C_i^{\beta}$ for this procedure can be appreciated from Figure 4 (top) where an example involving the C^{β} signals of T37 and of the next two residues, N38 and K39, is shown. The neighbours of A11 and T32, that is L10, L12 and L31, L33, respectively, were identified in a similar manner. By a detailed investigation of all possible correlations it was thus possible to assign the sequence fragments L8 – L12, K18 – W42 and R49 – L61.

Further assignments were obtained by exploiting those cross peaks in the NCA and NCO region of NCACX and NCOCX spectra that had not been used yet. An example is the assignment of the fragment Y13-D14-Y15-Q16. Possible candidates for the tyrosines, the glutamine and the aspartic acid were identified after inspection of the not yet assigned signal sets. Four of these signal patterns showed matching cross peaks of the type $N_iC_i^{\alpha}$ and $N_{i+1}C_i^{\alpha}$ and the respective carbonyl analogues that we were able to connect. An assignment at an earlier stage was difficult, because the corresponding residues showed insufficient transfer between C^{α} and C^{β} in the NCOCX spectrum and the NCACX-PDSD spectrum. However, their signal patterns could be identified in the NCACX-BD spectrum, leading to an unequivocal assignment.

Signal sets for the remaining glutamic acids E7 and E17 were already identified in the PDSD spectrum at an earlier stage, while the assignment of their carbonyl signals was not yet achieved. However, only one unassigned NCO cross peak was left at the nitrogen chemical shift of K18, the amino acid following E17, yielding the required assignment. The assignment of this cross peak at $\delta = 123.4/174.4$ to $N_{K18}CO_{E17}$ was supported by the cross peaks $N_{K18}C_{E17}^{\alpha}$ and $N_{K18}C_{E17}^{\beta}$, which were found in the NCOCX spectrum. The nitrogen chemical shift of E17 at $\delta = 122.0$ was identified after searching in the NCACX-PDSD spectrum for cross peaks with the above-mentioned carbon chemical shifts. This assignment was confirmed by the cross peaks $N_{E17}CO_{Q16}$, $N_{E17}C_{Q16}^{\alpha}$ and $N_{E17}C_{Q16}^{\beta}$ observed in the NCOCX spectrum. Similarly, the nitrogen chemical shift of L8 was determined by utilising not yet assigned cross peaks of the type $N_{i+1}CO_i$ and $N_{i+1}C_i^{\alpha}$. The nitrogen chemical shift of E7 was then deduced from the cross peaks $N_{E7}CO_{E7}$, $N_{E7}C_{E7}^{\alpha}$ and $N_{E7}C_{E7}^{\beta}$.

In a previous paper[21] we have pointed out that signals from the N-terminal residues are weak or missing. The completion of

the assignment of the well-observable peaks corroborates this observation, since signals that could be used for the assignment of the N-terminal residues M1, D2, E3, T4, G5 and K6 and the C-terminal residue D62 were absent. In particular, we could not observe a fourth threonine signal set (Figure 3), only two glycine peaks instead of three in the NCA spectrum (Figure 2), and no correlation between a glycine and a threonine, which should be readily observable given the quality of the NCOCX spectrum. Further problems occurred in the region V46 – N47. A potential valine side-chain signal pattern occurred in RFDR and PDSD spectra. However, it showed only broad signals with roughly less than one fifth of the integrated intensity observed for signals in other valine patterns. Hence, insufficient transfer in the NCACX and NCOCX spectra was observed for V46, and consequently no correlation could be established to N47 and E45. Also, the aromatic carbons of Y13 and Y15 could not be assigned. The observed signal loss could be attributed to dynamic processes, for example involving ring flips. The chemical shifts of the assigned signals are listed in Table 1.

Discussion

The observable ^{13}C and ^{15}N signals of the 62-residue α-spectrin SH3 domain in the precipitated form have been assigned by 2D magic angle spinning NMR. This assignment comprises all except five residues of the domain and may provide a basis for determining its structure in the solid state. The analysis is valid for one fully reproducible type of sample preparation for the α-spectrin SH3 protein construct used. The concept presented here can be readily transposed to larger proteins by trivial execution of the NCACX and NCOCX techniques in a three-dimensional manner, and by application of other C – C mixing units, for example the SPC-5 sequence[10] in the NCACX and NCOCX pulse sequences. For much larger protein systems such as membrane proteins, additional resolving power is expected from the exploitation of proton chemical shifts or $^{1}H - ^{13}C$ or $^{1}H - ^{15}N$ heteronuclear dipolar couplings for the generation of genuine triple-resonance 3D spectra.

In this study, it is demonstrated that assignment strategies in the solid state benefit strongly from selective transfer that directs the polarisation in a defined and efficient manner along the characteristic $^{15}N,^{13}C$ spin topology networks in the polypeptide chain. In particular, discrimination of inter- or intraresidue contacts in $^{15}N - ^{13}C$ backbone correlations proved to be vital for an unequivocal assignment of NCO-type cross peaks. An example are correlations between the amide nitrogen atom (residue *i*), the carbonyl carbon atom and α-carbon atom signals of the previous amino acid (residue $i-1$) in the NCOCX spectra, that may be "impure" and more difficult to interpret if during the nitrogen – carbonyl transfer period spurious excitation of the α-carbon atom or carbonyl group of residue *i* by the r.f. field takes place because of the competing N_iCO_{i-1} and $N_iC_i^{\alpha}$ or N_iCO_i transfers. This situation is very similar to the liquid state, where selective transfers ensure high sensitivity and simple interpretation of the spectra.

The assignment process would profit from a uniform, chemical shift range independent carbon – carbon transfer in the NCACX and NCOCX sequences. The implementation of other existing carbon – carbon transfer techniques such as SPC-5 or of newly developed ones into the NCACX and NCOCX sequences are planned. Our choice was dictated by the experimental constraints that are associated with biological samples. In particular, further attempts to increase the observed resolution must minimise any additional thermal and mechanical stress applied to the sample. Spinning frequency, decoupling power and the B_1 field strength applied during mixing periods had to be adjusted such that the samples remained stable while spectra with sufficient resolution were obtained. In this context, spinning frequencies of 8 kHz, decoupling fields of 70 kHz, sample cooling to 278 K and the combination of previously described pulse sequences appeared to be most practical. Otherwise a substantial broadening of the NMR signals was observed.

There are several possible explanations for the absence of signals from the first six N-terminal and the last C-terminal residues, from V46, N47, from tyrosine side chains of Y13 and Y15 and from the side chain of K39 in the presented spectra. In solution, the N terminus is flexible, leading to stronger signals than observed for the globular part of the protein. On the contrary, these signals seem strongly attenuated or absent in the spectra of our solid sample. One reason may be the flexibility of the N terminus, which could be on a time scale that interferes with the proton decoupling. As a result, the desired line narrowing is not realised. At same time the efficiency of cross polarisation is reduced for mobile protein segments. Another explanation for the missing signals relates to the occurrence of heterogeneous broadening which may result from a multitude of conformers that are "frozen out" upon precipitation during the preparation of the solid sample. This leads to increased chemical shift dispersion for the signals of the involved residues and cannot be removed by decoupling techniques. Further insight might be gained from measurements at low temperature and from relaxation studies.

We hope that the strategies presented here will pave the way for studies on ligands bound to membrane-embedded proteins by MAS solid-state NMR. In our study, narrow lines were obtained for the well-ordered globular part of the protein. The peptide ligands bound to G-protein-coupled receptors are expected to adopt a rigid structure by the action of the protein scaffold and should hence show well-resolved spectra that are straightforward to analyse. We expect also spectra of similar quality for the transmembrane regions of membrane proteins, except their lipid-exposed side chains, since both Fischer et al.[37] and van Rossum et al.[38] previously reported on comparable ^{13}C line widths of the reaction centre of the photosynthetic bacterium *Rhodobacter sphaeroides*, a transmembrane complex.

Materials and Methods

Expression of the α-spectrin SH3 protein: Plasmid pET3d coding for α-spectrin SH3 protein from chicken brain was a generous gift of Dr. M. Saraste, EMBL (Heidelberg, Germany). The SH3 protein was expressed in *Escherichia coli*, using a minimal medium based on M9 salts. 2 g [u-^{13}C]glucose and 1.0 g $^{15}NH_4Cl$ per litre of medium were added in the case of the uniformly $^{13}C,^{15}N$-labelled SH3 domain.

Table 1. ^{13}C and ^{15}N chemical shift values (δ) of the precipitated α-spectrin SH3 domain.

Residue	^{15}N	^{13}CO	$^{13}C^{\alpha}$	$^{13}C^{\beta}$	$^{13}C^{\gamma}$	$^{13}C^{\delta}$	$^{13}C^{\varepsilon}$	$^{13}C^{\eta}$	$^{13}C^{\zeta}$
E7	122.0	176.2	55.9	31.2	36.4				
L8	121.5	176.9	53.0	46.0	26.5	23.5/22.6			
V9	110.9	172.6	57.3	35.7	23.7/20.4				
L10	123.7	176.4	52.8	46.6	27.4	26.4/24.2			
A11	127.5	177.9	52.4	19.8					
L12	127.8	174.9	55.9	43.1	26.7	25.4/21.9			
Y13	110.0	173.8	55.2	43.5					
D14	117.4	176.5	54.6	41.8					
Y15	118.6	172.8	60.1	43.5					
Q16	126.5	174.0	53.8	29.6	33.8				
E17	122.0	174.4	55.7	33.4	37.3				
K18	123.4	174.6	55.0	34.8	26.2	29.4	42.0		
S19	111.3	173.3	56.5	63.7					
P20	137.2	177.0	65.0	32.1	27.3	50.1			
R21	112.0	175.2	55.2	34.1	27.2	43.9			
E22	119.3	174.8	54.8	33.9	37.5				
V23	112.2	172.0	59.1	35.0	21.3/19.8				
T24	116.4	174.3	61.8	71.8	21.3				
M25	121.1	173.5	53.8	36.4	31.7				
K26	125.0	174.9	53.7	34.2	24.4	28.8	42.0		
K27	122.2	177.9	58.5	32.5	24.3	29.7	42.0		
G28	116.3	173.9	44.6						
D29	121.8	175.0	55.1	42.2					
I30	119.8	176.7	58.3	35.9	26.8/18.1	11.4			
L31	128.4	177.0	53.3	42.5	28.1	27.4/26.4			
T32	118.8	173.8	62.7	69.8	22.5				
L33	130.1	174.4	55.0	43.0	26.8	25.5/23.8			
L34	125.7	177.6	55.0	43.0	26.8	26.0/22.2			
N35	113.9	174.6	54.4	41.5					
S36	124.8	173.5	56.8	62.0					
T37	112.6	175.7	65.0	70.9	21.6				
N38	126.0	174.8	54.0	41.6					
K39	121.4	176.2	58.2	33.4					
D40	115.3	177.2	55.7	44.4					
W41	122.7	174.2	55.9	32.9	111.0	128.5/128.5	139.0/118.7	114.8/121.0	125.7
W42	123.6	174.8	53.5	31.6	112.2	126.1/129.3	139.3/121.1	114.7/119.9	124.3
K43	119.6	174.8	54.0	33.8	24.2	29.3	42.0		
V44	121.9	173.1	59.3	36.4	21.0/18.6				
E45	120.0	175.5	56.1	30.9	34.8				
V46			59.9	33.1	20.8/19.8				
N47		177.5	55.0						
D48	113.9	174.6	54.1	40.5					
R49	122.2	176.6	55.2	34.1	27.2	43.9			
Q50	116.6	175.9	53.1	31.6	33.3				
G51	106.8	170.5	45.9						
F52	118.6	175.3	58.8	42.5	140.2	131.5/131.5	131.4/131.4		129.3
V53	110.0	172.6	57.9	33.5	22.3/17.0				
P54	136.8	177.7	61.6	30.1	28.3	50.0			
A55	129.0	178.7	54.0	15.9					
A56	113.0	177.7	52.8	18.2					
Y57	113.4	174.4	54.8	37.2	133.3	118.5	130.8		159.5
V58	110.7	173.8	57.8	35.5	22.4/19.8				
K59	119.6	176.4	54.0	37.2	24.7	29.6	42.0		
K60	126.7	176.6	58.4	33.4	26.0	29.6	42.0		
L61	125.7	175.6	54.3	41.4	29.4	26.6/23.0			
D62									

Preparation of the protein sample for MAS measurements: A 200-mM $(NH_4)_2SO_4$ solution (pH 3.5, 0.04% (w/v) NaN_3) was added to a 33-mM solution of the SH3 domain (pH 3.5), at a volume ratio of 1:1. The SH3 domain was precipitated by changing the pH value of the mixture to 7.5 in an NH_3 atmosphere. The solution was kept at 4 °C for three days before the precipitate was separated by centrifugation (20 min, 15000 rpm). In this form, approximately 10 mg protein was transferred into a 4-mm CRAMPS rotor. The core of the upper spacer of the CRAMPS rotor was closed in order to maintain a constant level of water inside.

NMR spectroscopy: The NMR measurements were recorded on a Bruker DMX750 spectrometer using double-channel and triple-channel CP-MAS probeheads. The spinning frequency of the 4-mm ZrO_2-CRAMPS rotors was stabilised to ± 2 Hz. The RFDR spectra were acquired at a radio frequency of 188.6 MHz, and a spinning

frequency of 8 kHz using TPPI[34] for phase sensitive detection.[22] The 90-degree proton pulse was set to 2.5 μs, ^{13}C B_1 fields of 50 kHz during the ramped CP sequence with a mixing time of 0.5 ms were used, and a 100%/50% ramp was applied on the proton channel. Rotor-synchronised π-pulses with a length of 21 μs were applied during the RFDR mixing time of 1 ms or 3 ms.

For the standard proton-driven spin diffusion experiments similar parameters were used; but with the carbon $\pi/2$ pulse length changed to 4.9 μs. The proton decoupler was switched off during the spin diffusion period of 5 ms and 15 ms.

All triple-resonance NMR spectra were recorded using an MAS frequency of 8 kHz while stabilizing the sample temperature at 278 K. ^{15}N polarisation was created with a ramped CP matching[35, 36] and an HN contact time of 2 ms. For all experiments, HN matching was first optimised using CW fields at the +1 sideband of the Hartmann–Hahn CP matching curve. ^{1}H and ^{15}N r.f. fields during transfer were chosen to be 40 and 32 kHz, respectively. For band-selective SPECIFIC CP transfer[6] from nitrogen atoms to carbon atoms, the ^{13}C carrier frequency was placed slightly outside the chemical shift range of the CO (for NCO) or of the C^{α} (for NCA transfer) signals, respectively. R.f. fields during the NC contact were chosen to be 30 kHz and 15 kHz for ^{15}N and ^{13}C irradiation, respectively. Mixing times between 2 and 4 ms and linear ramps from 100 to 80% on the ^{15}N r.f. field were employed to optimise efficiency and selectivity of the transfer. For all experiments involving homonuclear spin diffusion transfer, ^{13}C r.f. fields of 50 kHz were used to excite or reconvert longitudinal magnetisation before and after the $^{13}C-^{13}C$ mixing time. BASE-DREAM $C^{\alpha}C^{\beta}$ experiments were performed by using ramped ^{13}C r.f. amplitudes and by placing the carrier frequency in the middle of the C^{α} and C^{β} signals. With a MAS frequency of 8 kHz, a linear modulated r.f. field between 6 and 3 kHz results in a band-selective excitation profile of $\delta = 25-35$. 128 (NCO, NCA) or 196 (NCOCX, NCACX) t_1 experiments were recorded in phase-sensitive mode using a TPPI scheme. Linear prediction in t_1 was performed during data processing. In all experiments, two-pulse phase modulation (TPPM)[39] was applied to decouple protons in t_1 and t_2, applying 7-μs proton pulses (with a flip angle of 170°), and $\pm 15°$ phase shifts.

Support from the DFG (SFB 449), the NWO (PIONIER) and from the EU (BIO4-CT97-2101) is gratefully acknowledged. We thank Kristina Rehbein for the preparation of the protein samples. J.P. is supported by the HSPIII.

[1] E. R. Andrew, A. Bradbury, R. G. Eades, *Nature* **1958**, *182*, 1659.
[2] I. J. Lowe, *Phys. Rev. Lett.* **1959**, *2*, 285.
[3] J. Schaefer, E. O. Stejskal, J. R. Garbow, R. A. McKay, *J. Magn. Reson.* **1984**, *59*, 150–156.
[4] B. Q. Sun, P. R. Costa, R. G. Griffin, *J. Magn. Reson.* **1995**, *112*, 191–198.
[5] M. Baldus, D. G. Geurts, S. Hediger, B. H. Meier, *J. Magn. Reson.* **1996**, *118*, 140–144.
[6] M. Baldus, A. T. Petkova, J. Herzfeld, R. G. Griffin, *Mol. Phys.* **1998**, *95*, 1197–1207.
[7] A. E. Bennett, J. H. Ok, R. G. Griffin, S. Vega, *J. Chem. Phys.* **1992**, *96*, 8624–8627.
[8] M. Baldus, M. Tomaselli, B. H. Meier, R. R. Ernst, *Chem. Phys. Lett.* **1994**, *230*, 329–336.
[9] B. Q. Sun, P. R. Costa, D. Kocisko, P. T. Lansbury, R. G. Griffin, *J. Chem. Phys.* **1995**, *102*, 702–707.
[10] M. Hohwy, C. M. Rienstra, C. P. Jaroniec, R. G. Griffin, *J. Chem. Phys.* **1999**, *110*, 7983–7992.
[11] A. Brinkmann, M. Eden, M. H. Levitt, *J. Chem. Phys.* **2000**, *112*, 8539–8554.
[12] G. T. Montelione, G. Wagner, *J. Magn. Reson.* **1990**, *87*, 183–188.
[13] L. E. Kay, M. Ikura, R. Tschudin, A. Bax, *J. Magn. Reson.* **1990**, *89*, 496–514.
[14] G. M. Clore, A. M. Gronenborn, *Prog. NMR Spectrosc.* **1991**, *23*, 43–92.
[15] J. Cavanagh, W. J. Fairbrother, A. G. Palmer III, N. J. Skelton, *Protein NMR Spectroscopy: Principles and Practice*, Academic Press, San Diego **1996**.
[16] M. Sattler, J. Schleucher, C. Griesinger, *Prog. NMR Spectrosc.* **1999**, *34*, 93–158.
[17] M. Lee, W. I. Goldburg, *Phys. Rev.* A **1969**, *140*, 1261–1271.
[18] A. Bielecki, A. C. Kolbert, M. G. Levitt, *Chem. Phys. Lett.* **1989**, *155*, 341–346.
[19] B. J. van Rossum, H. Förster, H. J. M. de Groot, *J. Magn. Reson.* **1997**, *124*, 516–519.
[20] N. Bloembergen, *Physica* **1949**, *15*, 386–426.
[21] J. Pauli, B. van Rossum, H. Foerster, H. J. M. de Groot, H.Oschkinat, *J. Magn. Reson.* **2000**, *143*, 411–416.
[22] G. J. Boender, J. Raap, S. Prytulla, H. Oschkinat, H. J. M. de Groot, *Chem. Phys. Lett.* **1995**, *237*, 502–508.
[23] S. K. Straus, T. Bremi, R. R. Ernst, *J. Biomol. NMR* **1998**, *12*, 39–50.
[24] A. McDermott, T. Polenova, A. Bockmann, K. W. Zilm, E. K. Paulsen, R. W. Martin, G. T. Montelione, *J. Biomol. NMR* **2000**, *16*, 209–219.
[25] R. Verel, M. Baldus, M. Ernst, B. H. Meier, *Chem. Phys. Lett.* **1998**, *287*, 421–428.
[26] S. R. Hartmann, E. L. Hahn, *Phys. Rev.* **1962**, *128*, 2042–2053.
[27] A. Pines, M. G. Gibby, J. S. Waugh, *J. Chem. Phys.* **1973**, *59*, 569–590.
[28] A. Kubo, C. A. McDowell, *J. Chem. Soc.* **1988**, *84*, 3713–3730.
[29] D. P. Raleigh, M. H. Levitt, R. G. Griffin, *Chem. Phys. Lett.* **1988**, *146*, 71–76.
[30] M. G. Colombo, B. H. Meier, R. R. Ernst, *Chem. Phys. Lett.* **1988**, *146*, 189–196.
[31] N. C. Nielsen, H. Bildsoe, H. J. Jakobsen, M. H. Levitt, *J. Chem. Phys.* **1994**, *101*, 1805–1812.
[32] J. R. Long, B. Q. Sun, A. Bowen, R. G. Griffin, *J. Am. Chem. Soc.* **1994**, *116*, 11 950–11 956.
[33] D. C. Maus, V. Copie, B. Sun, J. M. Griffiths, R. S. Griffin, S. Luo, R. R. Schrock, A. H. Liu, S. W. Seidel, W. M. Davis, A. Grohmann, *J. Am. Chem. Soc.* **1996**, *118*, 5665–5671.
[34] R. R. Ernst, G. Bodenhausen, A. Wokaun, *Principles of Nuclear Magnetic Resonance in One and Two Dimensions*, Clarendon, Oxford, **1987**.
[35] G. Metz, X. L. Wu, S. O. Smith, *J. Magn. Reson.* **1994**, *110*, 209–227.
[36] S. Hediger, B. H. Meier, R. R. Ernst, *Chem. Phys. Lett.* **1995**, *240*, 449–456.
[37] M. R. Fischer, H. J. M. de Groot, J. Raap, C. Winkel, A. J. Hoff, J. Lugtenburg, *Biochemistry* **1992**, 11 038–11 049.
[38] B. J. van Rossum, J. Wachtveitl, J. Raap, K. van der Hoef, P. Gast, J. Lugtenburg, D. Oesterhelt, H. J. M. de Groot, *Spectrochim. Acta Part A* **1997**, *53*, 2201–2208.
[39] A. E. Bennett, C. M. Rienstra, M. Auger, K. V. Lakshmi, R. G. Griffin, *J. Chem. Phys.* **1995**, *103*, 6951–6958.

Received: July 18, 2000 [F98]